Extended Abstracts of the 2006 International Conference on Solid State Devices and Materials, Yokohama, 2006, pp. 704-705

P-8-16

# $TiO_2$ nanocrystal prepared by ALD system at elevated temperature

C. H. Lin, C. C. Wang, P. J. Tzeng, S. Maikap, H. Y. Lee, L. S. Lee, and M.-J. Tsai
Electronics and Opto-Electronics Research Laboratories
Industrial Technology Research Institute
Chutung, Hsinchu 310, Taiwan
Phone : 886-3-5917148, Fax : 886-3-5917690
E-mail : linchahsin@itri.org.tw

## 1. Abstract

The $TiO_2$ nanocrystals were successfully fabricated using an ALD system. The TiN/$Al_2O_3$ laminated structure was employed as the starting structure and after appropriate annealing process, the TiN would be oxidized and $TiO_2$ nanocrystals were formed. Experimental results indicated that the rapid thermal annealing (RTA) temperature was very critical. Also, the thickness of each TiN layer in the TiN/$Al_2O_3$ laminated starting structure was also crucial for the $TiO_2$ nanocrystal formation.

## 2. Introduction

Recently, nanocrystal charge trapping layer for non-volatile memory application was widely investigated due to the 3-D charge confined structure that has a great potential to become the mainstream of the next generation non-volatile memory [1-2]. In the past, sputter system was widely adopted to fabricate nanocrystal, such as W or Ni nanocrystal [3-4], however, precisely thickness control is more difficult for sputter and this would cause large nanocrystal size distribution. Atomic-layer-deposition (ALD) in nature has a better thickness-control ability due to the self-limited reaction mechanism. In this study, ALD system was employed to fabricate $TiO_2$ nanocrystal scattered in the $Al_2O_3$ film. The high crystallization temperature of $Al_2O_3$ film could restrain additional leakage path formation during the annealing process. Also, the conduction band offset between $TiO_2$ and $Al_2O_3$ is around 1.8 eV and would be beneficial for charge retention.

## 3. Experimental results and discussions

Figure 1 shows the schematic diagrams of the employed TiN/$Al_2O_3$ laminated structures. For samples A and B, the thickness of TiN layer in each TiN/$Al_2O_3$ laminated period was 0.5 and 1 nm respectively. Figure 2 shows the atomic force microscopy (AFM) topography of sample A with and without various annealing conditions. For figures 2(b) and 2(c), the flatter surface indicated that 550°C and 750°C are not enough for nanocrystal (grain growth) formation. Figure 3 shows the comparison of AFM topography of samples A and B after 950°C ($N_2$) annealing process. Both higher annealing temperature and thicker TiN layer [Fig. 3(b)] would result in the rougher surface. The rougher surface of Fig. 3(a) is resulted from the formation of nanocrystal. During the high-temperature annealing, TiN layer would be oxidized to form $TiO_2$. TiN is easily oxidized since $TiO_2$ is the thermodynamically stable phase, and hence, the trace $O_2$ in the RTA ambiance is enough to oxidize TiN layer [5]. For sample B [Fig. 3(b)], the rougher surface is resulted from TiN deformation and grain growth of the $TiO_2$ layer [5]. For this phenomenon, we will discuss in detail later.

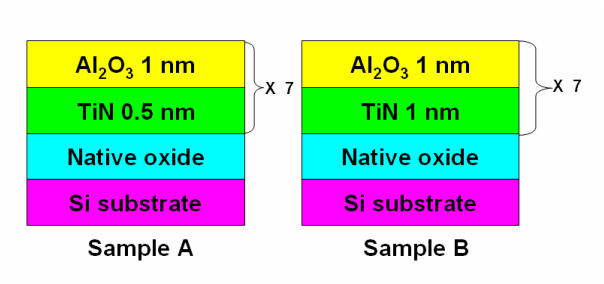


Fig. 1 schematic diagrams of the employed TiN/$Al_2O_3$ laminated structures.

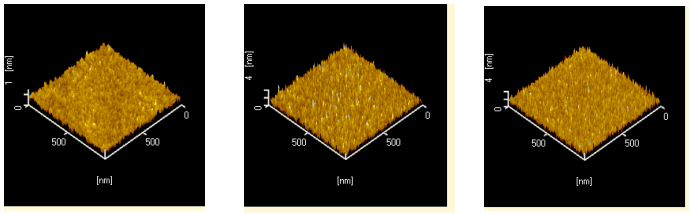

(a) (b) (c)

Fig. 2 AFM topography of Sample A with and without various RTA processes ; (a): as-deposited, Ra = 0.115 nm, (b): 550°C, 2 min, in $N_2$, Ra = 0.332 nm, (c): 750°C, 2 min, in $N_2$, Ra = 0.346 nm.

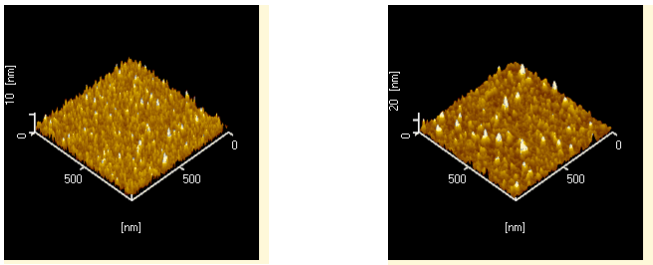

(a) (b)

Fig. 3 AFM topography of (a) Sample A, and (b) Sample B after 950°C, 2 min, in $N_2$ annealing (Sample A : Ra = 0.839 nm, Sample B : Ra = 2.18 nm).

Figure 4 shows the high-resolution transmission electron microscopy (HR-TEM) micrograph of Sample A after 950°C, 2 min, in $N_2$ annealing. Many nanocrystals are scattered in the $Al_2O_3$ layer. The diameters of these nanocrystals distribute between ~2 nm to ~6 nm.

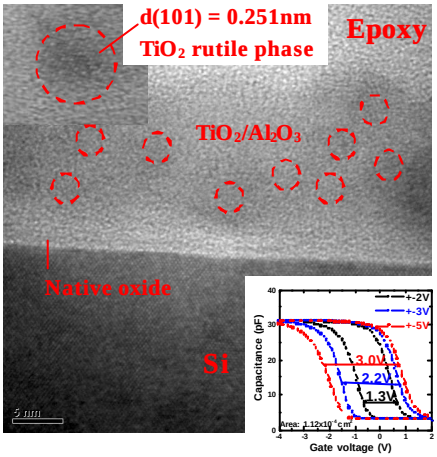


Fig. 4 HR-TEM micrograph of Sample A after RTA (950°C, 2 min, $N_2$). The inset shows the C-V characteristics of sample with this kind of charge trapping layer.

Figure 5 shows the HR-TEM micrograph of Sample B after 950°C, 2 min, in $N_2$ annealing. A large grain could be observed as indicated between arrows (1)~(3). The formation of large grains may be due to abnormal growth to reduce the surface energy of $TiO_2$ layer. Also, the large grains would result in the much rougher surface, as indicated in arrow (2) of Fig. 5. For the device fabrication, a blocking oxide layer was deposited onto the nanocrystal charge trapping layer to ensure good charge retention characteristic. The rougher surface could damage the blocking oxide and might cause serious back injection current from the gate. This can lead to poor characteristic of charge retention.

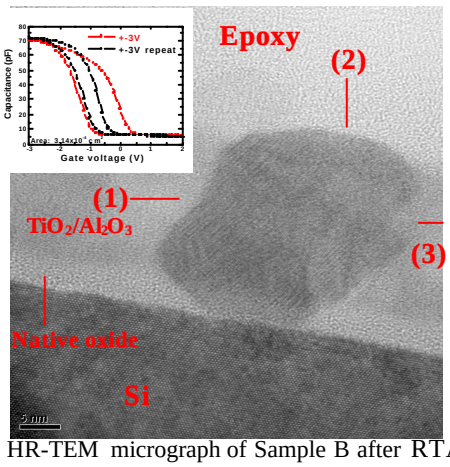


Fig. 5 HR-TEM micrograph of Sample B after RTA (950°C, 2 min, $N_2$). The inset shows the C-V characteristics of sample with this kind of charge trapping layer.

Figures 6 and 7 depict the X-ray photoelectron spectroscopy (XPS) spectra of Samples A and B after 950°C, 2 min, in $N_2$ annealing. The Al binding signals [Figs. 6(a) and 7(a)] indicated that the $Al_2O_3$ film was not destroyed, however, the Ti-N binding signal (455.8 eV) was not observed and TiN fully oxidized, as shown in Figs. 6(b) and 7(b). Compared with TEM result, it is believed that the $TiO_2$ nanocrystal was formed successfully.

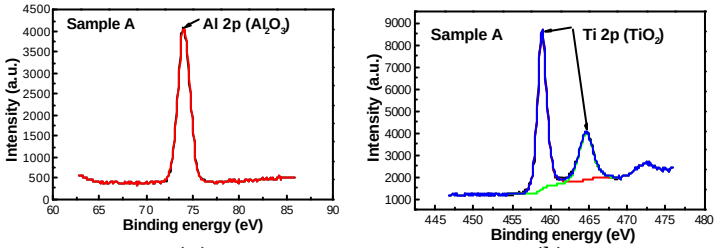


(a) (b)

Fig. 6 XPS spectra of Sample A, (a) Al 2p signal; (b) Ti 2p signal.

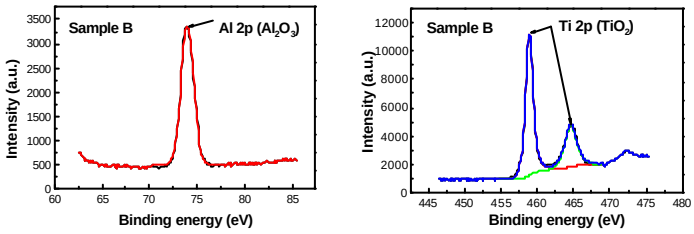


(a) (b)

Fig. 7 XPS spectra of Sample B (a) Al 2p signal; (b) Ti 2p signal.

## 4. Conclusion

The effects of annealing temperature and TiN thickness in the TiN/$Al_2O_3$ laminated period on the formation of $TiO_2$ nanocrystal were studied. Experimental results indicated that high temperature annealing and thinner TiN layer (< 1 nm) could facilitate the $TiO_2$ nanocrystal growth. The thicker TiN layer would lead to too large grains and the lower annealing temperature could not supply enough energy for $TiO_2$ nanocrystal nucleation.

### References


[1] C. Lee, A. Gorur-Seetharam, and Edwin C. Kan, IEDM (2003) 557.

[2] J. J. Lee, Y. Harada, J. W. Pyun, and D. L. Kwong, Appl. Phys. Lett. **86** (2005) 103505.

[3] Z. Tan, S. K. Samanta, W. J. Yoo, and S. Lee, Appl. Phys. Lett. **86** (2005) 013107.

[4] S. K. Samanta, W. J. Yoo, G. Samudra, E. S. Tok, L. K. Bera and N. Balasubramanian, Appl. Phys. Lett. **87** (2005) 113110.

[5] C. H. Lin, C. C. Wang, P. J. Tzeng, C. S. Liang, W. M. Lo, H. Y. Li, L. S. Lee, S. C. Lo, Y. W. Chou, and M-J Tsai, SSDM (2005) 62.